Received: 5 August 2021 | Revised: 22 November 2021 | Accepted: 25 November 2021

DOI: 10.1111/ppl.13607

UPTAKE, TRANSPORT AND ASSIMILATION

Physiologia Plantarum

Nodulating white lupins take advantage of the reciprocal interplay between N and P nutritional responses

Sara Buoso[1] | Anita Zamboni[2] | Alessandro Franco[1] | Mauro Commisso[2] | Flavia Guzzo[2] | Zeno Varanini[2] | Roberto Pinton[1] | Nicola Tomasi[1] | Laura Zanin[1]

[1]Department of Agricultural, Food, Environmental and Animal Sciences, University of Udine, Udine, Italy

[2]Department of Biotechnology, University of Verona, Verona, Italy

Correspondence
Laura Zanin, Department of Agricultural, Food, Environmental and Animal Sciences, University of Udine, Via delle Scienze 206 - 33100 Udine, Italy.
Email: laura.zanin@uniud.it

Edited by J.K. Schjoerring

Abstract

The low bioavailability of nutrients, especially nitrogen (N) and phosphorus (P), is one of the most limiting factors for crop production. In this study, under N- and P-free nutrient solution (−N−P), nodulating white lupin plants developed some nodules and analogous cluster root structures characterized by different morphological, physiological, and molecular responses than those observed upon single nutrient deficiency (strong acidification of external media, a better nutritional status than −N+P and +N−P plants). The multi-elemental analysis highlighted that the concentrations of nutrients in white lupin plants were mainly affected by P availability. Gene-expression analyses provided evidence of interconnections between N and P nutritional pathways that are active to promote N and P balance in plants. The root exudome was mainly characterized by N availability in nutrient solution, and, in particular, the absence of N and P in the nutrient solution triggered a high release of phenolic compounds, nucleosides monophosphate and saponines by roots. These morphological, physiological, and molecular responses result from a close interplay between N and P nutritional pathways. They contribute to the good development of nodulating white lupin plants when grown on N- and P-free media. This study provides evidence that limited N and P availability in the nutrient solution can promote white lupin-*Bradyrhizobium* symbiosis, which is favourable for the sustainability of legume production.

1 | INTRODUCTION

Phosphorous (P), next to nitrogen (N), is one of the main limiting nutrients for crop productivity. The improvement of P use efficiency in plants is needed for a sustainable agriculture, mainly because (1) the phosphate rock used to manufacture P fertilizers is a non-renewable resource, and (2) an excessive use of P fertilizers (along with organic manure) has a negative impact on the environment as it leads to the eutrophication of surface waters (Johnston et al., 2014; Syers et al., 2008). Therefore, it is important to identify new strategies for improving the usage of nutrients by plants.

There is great variability among legume species in their capacity to counteract low P availability (Le Roux et al., 2008). White lupin (*Lupinus albus* L.) is a Fabaceae species considered as a model plant for studying plant adaptation to low soil P environments, whereas its response to low N availability has been less investigated in the past years than in other Fabaceae plants (Le Roux et al., 2006; Le Roux et al., 2008; Schulze et al., 2006).

In P-depleted conditions, white lupin strongly modifies the root architecture with the formation of bottlebrush-like structures, so-called proteoid or cluster roots (Gardner et al., 1982; Shane & Lambers, 2005). These root structures are highly active at the metabolic level as a huge synthesis and release of exudates by white lupin roots into the rhizosphere has been described (Dinkelaker et al., 1989; Gardner et al., 1983; Neumann et al., 1999). White lupin exudome is mainly composed by citrate, malate and other carboxylates, as well as by phenolic compounds (such as genistein and its derivatives, like glycosylated and/or hydroxylated genistein). These root exudates strongly influence the biological and chemical properties of the rhizosphere (Neumann et al., 1999; Weisskopf et al., 2006). Moreover, the phosphate starvation response (PSR) refers to various morphological, biochemical and metabolic adaptations that cooperate to enhance P acquisition. Under P deficiency, plants increase the synthesis and secretion of organic acids, acid phosphatases (APs), and operate several metabolic bypasses to avoid P consumption (Liu et al., 2001; Plaxton & Tran, 2011; Tomasi et al., 2008; Vance et al., 2003). The release into the rhizosphere of a wide range of exudates is crucial for the effectiveness of the nutrient deficiency response. It leads to the mobilization of the sparingly available nutrients mainly via complexation, ligand exchange and, in the case of phenolic compounds, reduction (Cesco et al., 2010). Root exudates also affect soil microbial activities (Cesco et al., 2010).

Through the symbiosis interaction, Fabaceae species can self-provide sufficient N to satisfy their nutritional requirement. *Bradyrhizobium* spp. (*Lupinus*) are the soil-bacterial species most frequently infecting *Lupinus* plants and they induce the formation of root nodules (González-Sama et al., 2004; Jordan, 1984). It has been reported that the efficiency of the N_2-fixing process is sensitive to environmental limitations, especially nutritional disorders, which can impair the nodule activity (Chu et al., 2019; Qin et al., 2015). When P is limiting for plant growth, nodule activity is also affected, as the root metabolism is mainly dedicated to the synthesis and release in the rhizosphere of huge amounts of organic acids, as malate and citrate, acting to promote P-solubility in the soil. Under this condition, the activity of N assimilatory pathway and amino acid synthesis might be reduced while the synthesis of organic acids is promoted. Therefore, high malate concentration in nodulating P-deficient roots of white lupin was linked to a reduction of root nodules, N_2-fixation and synthesis of amino acids (Le Roux et al., 2006). The response of the individual partners involved in the symbiosis is important to redirect P fluxes in the organs when the nutrient is limiting in the external media. Indeed, nodules did not show any metabolic P-deficiency symptoms in comparison to roots under low P condition (Le Roux et al., 2006), becoming strong sink organs when P is limiting (Al-Niemi et al., 1997, 1998; Høgh-Jensen et al., 2002; Tang et al., 2001). In comparison to shoots and roots, nodules respond more slowly to fluctuations in P availability. Moreover, under low P conditions, nodulation promoted cluster roots formation in white lupin (Wang et al., 2019). This strategy seems to guarantee the acquisition of adequate P levels in nodules to meet the nutritional demand of rhizobial bacteroids (Le Roux et al., 2006; Thuynsma et al., 2014).

Numerous studies have separately investigated the physiological response to P supply and N_2 fixation in legume–rhizobium symbiosis; however, the reciprocal interaction between these two nutritional pathways is still obscure (for review, see Pueyo et al., 2021). A previous study on white lupin indicated changes in elemental composition when different P availability and nitrogen forms were applied to the nutrient solution (Sas et al., 2002). In particular, the authors observed that Fe and Mn levels in shoot and in the whole plant, respectively, increased in P-deficient plants rather than in P-sufficient ones and were even more concentrated when N was derived from N_2-fixation (Sas et al., 2002).

Understanding cross-connections among N-P nutritional pathways might be extremely useful to enhance biological N_2-fixation and maximize the efficiency of fertilization management. The aim of this work was to investigate putative synergisms between N and P nutrition that may play a crucial role for plant growth under low nutrient availability. The occurrence of cross-connections between the N-P nutritional pathways in nodulating white lupin plants was investigated through omic approaches, which allowed us to: (1) compare ionomic profile of nodulating white lupin plants, (2) monitor the expression of some genes involved in N-P nutritional pathways during the symbiosis, and (3) characterize the root exudome through an innovative approach (untargeted analyses).

2 | MATERIALS AND METHODS

2.1 | Plant growth

White lupin seeds (*L. albus* L. cv. Amiga; Südwestdeutsche Saatzucht, Rastatt, Germany) were soaked for 24 h in aerated water and germinated on a plastic net placed at the surface of an aerated 0.5 mM $CaSO_4$ solution in a growth chamber at 25°C in the dark. Thereafter, 4-day-old seedlings were transferred in a hydroponic system (six plants per pot), containing 2.2 L of a N- and P-free nutrient solution ("−N−P" treatment condition) with the following composition in μM: 1750 K_2SO_4, 1250 $MgSO_4$, 250 KCl, 25 H_3BO_4, 100 Fe(III)EDTA, 1.25 $MnSO_4$, 1.5 $ZnSO_4$, 0.5 $CuSO_4$, and 0.025 $Na_6Mo_7O_{24}$. The "−N+P" plants were grown in N- and P-free nutrient solution with the addition of 250 μM KH_2PO_4, the "+N−P" plants were grown in N- and P-free nutrient solution with the addition of 5000 μM $Ca(NO_3)_2$, whereas "+N+P" were grown in N- and P-free nutrient solution supplied with 5000 μM $Ca(NO_3)_2$ and 250 μM KH_2PO_4.The nutrient solutions were buffered at pH 6.0 by adding 0.5 mM 2-(*N*-morpholino) ethanesulfonic acid and were renewed every 3 days. A culture of *Bradyrhizobium* sp. (*Lupinus*) ISLU-16 (González-Sama et al., 2004) was grown in AG medium (Sadowsky et al., 1987) up to the exponential growth phase (10^8–10^9 cells ml^{-1}): 10 ml of liquid culture were pelleted at 3000*g*; the bacterial pellet was washed twice with sterile water and re-suspended in 1 ml of sterile water. Plant nutrient solutions were inoculated twice per week with *Bradyrhizobium*, prepared as previously described (1 ml of bacterial solution in 2.2 L of nutrient solution). Plants were grown in a growth chamber under controlled

conditions for 4 weeks (day/night photoperiod, 16/8 h; photosynthetically active radiation, 220 μmol m^{-2} s^{-1}; day/night temperature, 25/20°C; relative humidity, 70–80%). During the growth period, the light transmittance of leaves was monitored (SPAD-502, Minolta).

Molecular analyses were performed on the whole root system, collected at 14, 21, and 28 days after inoculation (DAI) with *Bradyrhizobium*. Fresh and dry weights (FW and DW, respectively), representative pictures, root external acidification, Fe(III)-chelate reductase activity, elemental analyses of white lupin plants and untargeted metabolomics of root exudates were performed at 28 DAI.

2.2 | Root external acidification by white lupin plants

The capacity of white lupin roots to acidify the external media was visualized on agar gel (0.9% w/v agar layer containing 0.04% w/v bromocresol purple, as pH indicator) as previously described by Buoso et al. (2021).

2.3 | Elemental analyses

The elemental composition of white lupin was analysed as previously described (Zanin et al., 2015; Zanin et al., 2017) by inductively coupled plasma mass spectrometry (ICP-MS NexION 300, PerkinElmer Inc.) and by CHN analyser (CHN IRMS Isoprime 100 Stable Isotope Ratio Mass Spectrometer, Elementar). For ICP analyses, shoots and roots were oven-dried at 60°C and samples were acid-digested with concentrated ultrapure HNO_3 (650 ml L^{-1}; Carlo Erba) using a single reaction chamber microwave digestion system (UltraWAVE, Milestone). Element quantifications were carried out using certified multi-element standards (CPI International, https://cpiinternational.com).

2.4 | RNA extraction and reverse transcription for real-time RT-PCR analyses

Real-time RT-PCR analyses were performed on white lupin roots as described by Zanin et al. (2018). Whole root systems of white lupin plants were sampled and RNA was extracted using Invisorb Spin Plant RNA kit (Stratec Molecular) following the manufacturer's instructions. The quality and quantity of RNA were checked by gel electrophoresis and by Nanodrop, respectively. cDNA was retrotranscribed using iScript Reverse Transcription Supermix for RT-qPCR (Bio-Rad Laboratories Inc.). Using Primer3 software (Koressaar & Remm, 2007; Untergrasser et al., 2012), primers were designed and synthesized by Sigma Aldrich (Table S1). The analyses were performed using CFX96 Real Time RT-PCR Detection (Biorad) and qPCR package for statistical R software (R version 3.5.1, www.dr-spiess.de/qpcR.html). For each primer pair, the efficiency of amplification was determined as indicated by Ritz and Spiess (2008). Data were referred to the averaged expression of three housekeeping genes coding for UBIQUITIN C (*LaUBC*), POLYPYRIMIDINE TRACT-BINDING PROTEIN (*LaPTB*), and HELICASE (*LaHEL*). Primers of the housekeeping genes were designed by Taylor et al. (2016). Data were normalized using the $2^{-\Delta\Delta CT}$ method (Livak & Schmittgen, 2001).

2.5 | Relative quantification of *Bradyrhizobium* in white lupin roots

Bradyrhizobium relative quantification was performed on white lupin roots by real-time RT–PCR, using primers specific for the *16S* rRNA gene of *Bradyrhizobium* (Chu et al., 2019). The expression of *16S* rRNA was then referred to the plant housekeeping gene *LaHEL* and data were normalized as reported for gene expression analyses.

2.6 | Fe(III)-chelate reductase activity of white lupin roots

The Fe(III)-chelate reductase activity of white lupin roots was evaluated by performing the bathophenanthroline-disulfonate assay at pH 5.5, as described in Zamboni et al. (2012). The absorbance of the solution was measured at 535 nm at intervals of 10 min (22.1 mM^{-1} cm^{-1} extinction coefficient).

2.7 | Untargeted metabolomics of root exudates

Three pools of plants (12 plants for each pool) per treatment were removed from the nutrient solution and roots were washed three times in deionized water. Then, the roots of each pool were submerged into 300 ml of deionized water, which was continuously aerated for 3 h. Solutions were filtered at 0.2 μm and immediately analysed. Then, 350 μl of solutions of root exudates were directly filtered with Minisart filters (pore size of 0.2 μm) and 10 μl were injected to the UPLC–MS system (UPLC Acquity I class on-line with a Xevo G2-XS mass spectrometer) equipped with a BEH C18 column (100 × 2.1 mm; 1.7 μm particle size). The chromatographic method was performed as described in a previous report (Commisso et al., 2019) with minor modifications. Briefly, solvent A consisted of water plus 0.1% formic acid and solvent B was 100% acetonitrile. The chromatographic gradient started with 0% B for 1 min; 40% B to 10 min; 70% B to 13.50 min; 99% B to 14.00 min; isocratic at 99% B to 16.00 min; 0% B to 16.10 min and isocratic at 0% B to 20 min. The flow rate was set at 0.350 ml min^{-1} and the column temperature was kept at 30°C. Samples were kept at 7°C. The Xevo G2-XS was equipped with an ESI ion source and metabolites were ionized in positive or negative mode. ESI parameters were the following: capillary voltage 0.8 kV, sampling cone 40 V, Source offset voltage 80 V, source temperature 120°C, desolvation temperature 500°C, cone gas (N) flow rate 50 L h^{-1}, and desolvation gas (N) flow rate 1000 L h^{-1}. Argon was used to fragment the ions by using collision-induced dissociation. Signals were acquired in continuum mode by using MassLynx software (Waters). An MS method including two scan functions was

created: the former recorded signals where ions were not fragmented, whereas in the latter the ions were fragmented by using relatively high energy set to 35 V. To achieve better information about the identity of the metabolites, some samples were submitted to further fragmentation analysis by changing the collision energy to lower value (15 V; low fragmentation force), whereas in others, the collision energy was increased to 45 V (high fragmentation force). The scan range was 50–2000 *m/z* and the scan speed was 0.3 s. Then, 100 pg μl^{-1} leucine-enkephalin solution (Waters) were injected with a constant flow rate of 10 $\mu l\ min^{-1}$ as lock mass calibrator. The sequence of samples was randomized. As control, blank samples (water LC–MS grade) were injected randomly during the experiment and at the beginning of the sample table.

2.8 | Metabolomics data processing and metabolite identification

Progenesis QI software (Waters) was exploited to process the raw MS data files. Two FQM (Feature Quantification Matrix, obtained by positive and negative ionization) were built by Progenesis QI (Waters, Nonlinear dynamics). The metabolite identification was performed by the following two strategies: (1) the *m/z* features of the datamatrices were compared to public databases (MassBank, PlantCyc, Plant Metabolic Network, and Human Metabolome Database), and the following parameters were used for the acceptance of the elemental composition: mass error ≤5 ppm and isotopic composition score (calculated by Progenesis QI) ≥95%; (2) a white lupin-specific in-house library of molecular masses was built, and mass error ≤7 ppm isotopic score and ≥90 were used for the acceptance of the elemental composition. For all the *m/z* features with elemental composition determined, the fragmentation spectrum obtained by ms/ms was inspected and compared with an in-house library of authentic standard, with public database (MassBank, MoNA, Metlin) and with the literature. Only in case of positive matching, the metabolites were putatively annotated. The data matrices including *m/z* features and the relative abundances were also subjected to multivariate statistical analyses: principal component analysis (PCA) and orthogonal partial least square discriminant analysis (OPLS-DA) through SIMCA 13.0 (Umetrics) after Pareto scaling and centring. For specific metabolites, univariate statistical analysis was performed by using a *t* test (p-value <0.05).

2.9 | Statistical analyses

Physiological, biochemical, and molecular analyses were performed on three independent biological replicates obtained from independent experiments ($n = 3$), a pool of six plants was used for each sample. Statistical significance was determined by one-way analysis of variance using Holm–Sidak test (p-value <0.05, $n = 3$) using SigmaPlot Version 12.0 software. The analyses of SPAD values were performed on 20 plants for each condition ($n = 20$).

Ionomic analysis was performed by using SIMCA P+ (Umetrics). Centring was applied to each dataset (nodule, root, and shoot). In order to define the number of latent components for OPLS(-DA) models, we applied partial cross-validation and a permutation test to highlight overfitting.

FIGURE 1 Representative pictures of shoots of white lupin plants after 28 days after inoculation (DAI) under the different nutrient conditions (+N+P, −N+P, +N−P, −N−P) and relative SPAD values (Holm–Sidak analysis of variance [ANOVA], for each condition 20 plants were analysed $n = 20$, p-value <0.05). Different letters indicate statistically significant differences

Regarding untargeted metabolomic analyses, root exudate was collected from 12 plants, and for each nutritional condition, 3 pools of plants were used ($n = 3$; for further details on the statistical parameters, refer to Section 2.8).

3 | RESULTS

3.1 | Morphological response

Under our conditions, the development of root nodules preceded of 1 week the formation of cluster roots (these latter developed 3 weeks after inoculation, from 21 DAI). At the end of the growing period (28 DAI), −N+P and +N−P showed typical symptoms ascribable to a low-nutrient availability: in −N+P, the leaves turned yellow, the number of nodules per plants increased, whereas the formation of cluster roots, acidification/alkalinization of external media, and blue/purple leaves occurred in +N−P (Figures 1, 2, S1, and S2). The −N−P condition was further characterized by a peculiar organ-morphogenesis, analogous structures of cluster roots (hereafter called "pseudo-cluster roots") developed along primary and secondary roots (Figures 2 and S1). These structures were morphologically different from the cluster roots developed under P-deficiency: lower root density and no classification in the known developmental stages of +N−P (juvenile, immature, mature and senescent developmental stages, Massonneau et al., 2001). No significant changes in the DW of white lupin plants were induced by treatments (Figures 3 and S2), although the FW increase under P deficiency (+N−P) and FW, DW and number of nodules per plant increased significantly in −N−P in comparison to +N+P plants (Figure S2). An intense acidification activity was observed in the root external solution surrounding the immature/mature cluster roots of P deficient plants (+N−P), while senescent clusters induced alkalinisation (Figure 2). In N-free nutrient solution, the whole root system showed acidification of the external media characterized by yellow spots close to nodules (pH less than 4.5). Furthermore, the lowest pH values were reached by roots of −N−P plants near the pseudo-cluster roots and nodules (in −N−P some of nodules clustered together along the primary root; the acidification of external media was estimated to be around 3.5–3.0 pH).

3.2 | Relative quantification of *Bradyrhizobium* on white lupin roots

The relative quantification of *Bradyrhizobium* in white lupin roots was performed at 14, 21, and 28 DAI. The *16S* rRNA abundance in root samples indicated the presence of live bacteria on white lupin roots. After 2 weeks from the inoculation, the same amount of *16S* rRNA was measured in plants regardless of the nutritional treatment. At 14 and 28 DAI, high expression values of ribosomal gene were observed in roots of plants grown without N in nutrient solution (−N+P and −N−P), although the double-stressed ones showed the highest values at both sampling times (Figure 3).

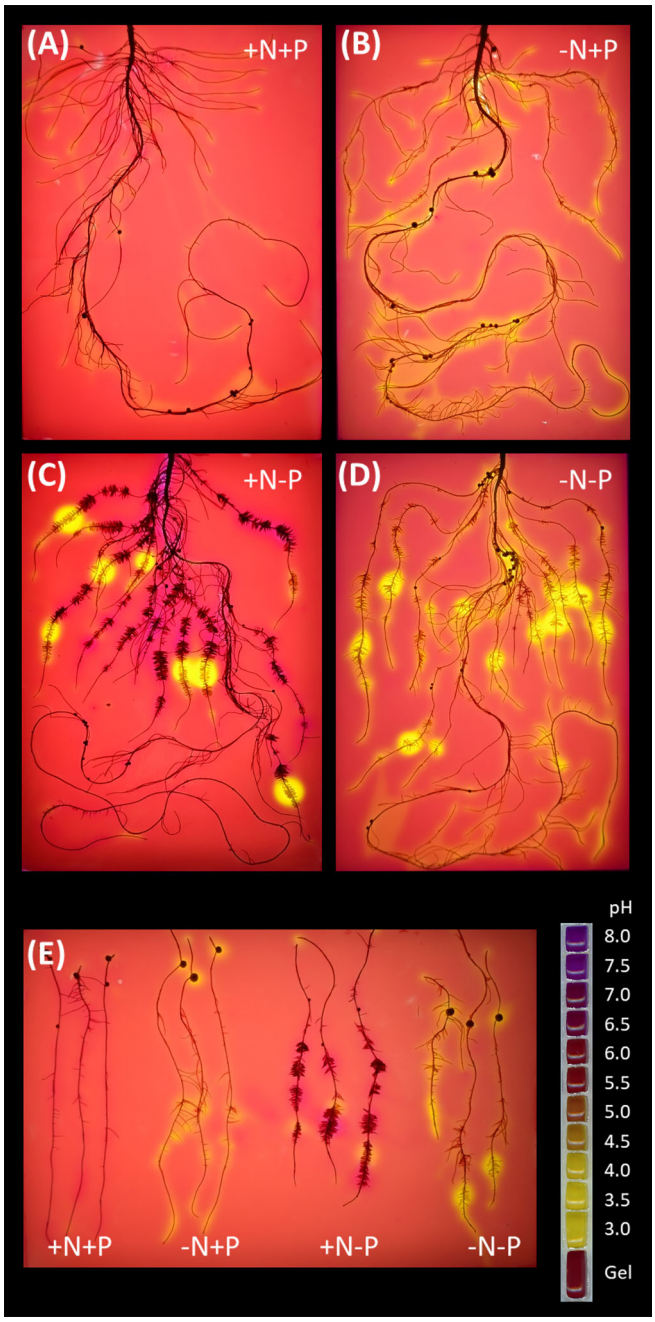

FIGURE 2 Acidification activity of white lupin roots using a pH gel indicator (bromocresol purple) at 28 days after inoculation (DAI) under the different nutrient conditions (+N+P, −N+P, +N−P, −N−P)

3.3 | Ionomic analysis

The macro- and micronutrient concentrations (Figures 3, S3, and S4, Table 1) determined in nodules, roots and shoots were analysed by multivariate statistics. Concerning nodules, PCA identified two main clusters depending on nutritional treatment (Figure 4). Through the first principal component, the white lupin nodules of plants grown in absence of P (+N−P and −N−P) were clearly separated from nodules of P-sufficient plants (+N+P and −N+P). Based on the results of this unsupervised analysis, and with the aim to identify variables

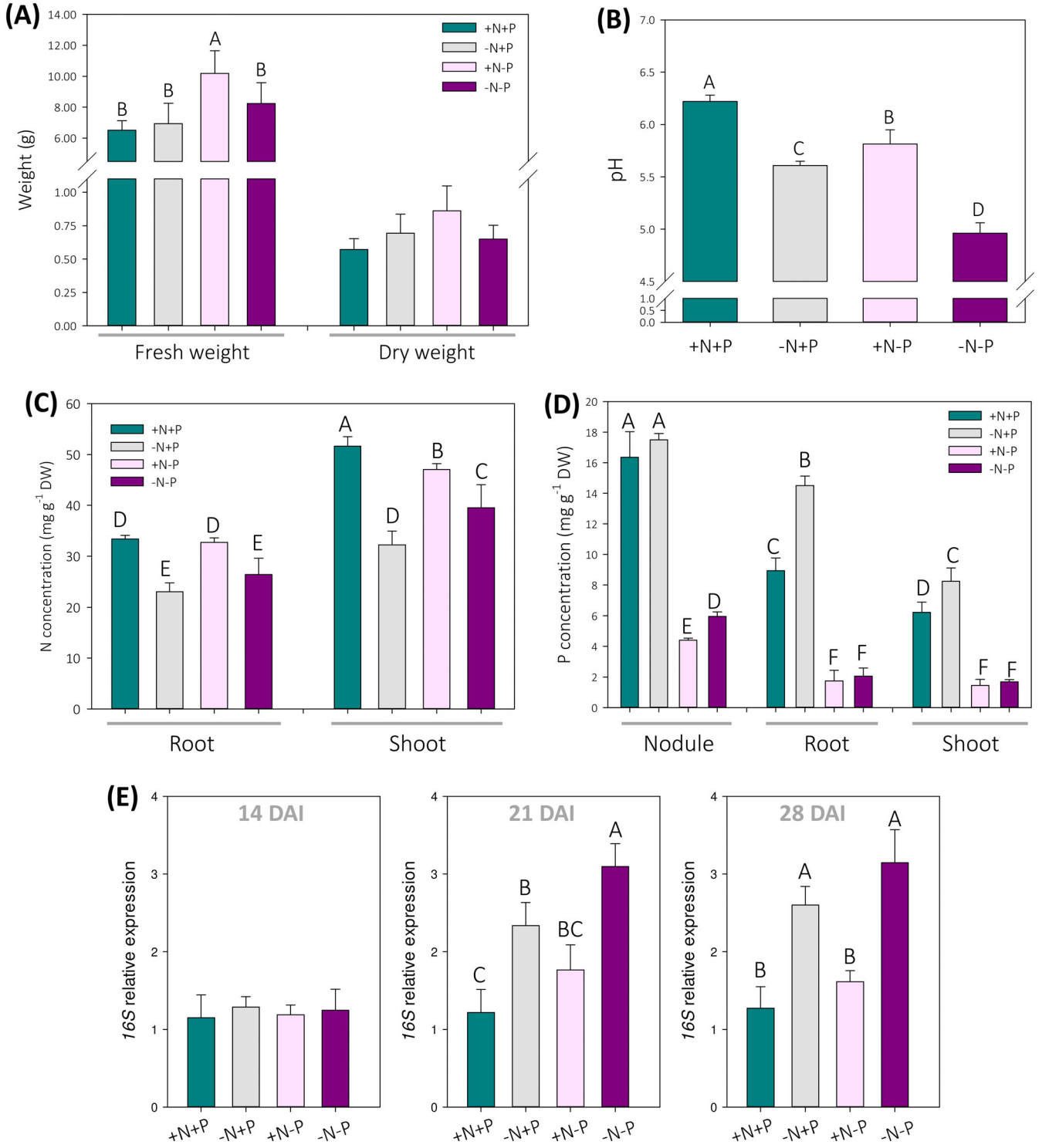

FIGURE 3 (A) Fresh and dry weights of nodulating white lupin plants at 28 days after inoculation (DAI) under different nutritional conditions (+N+P, −N+P, +N−P, −N−P). (B) pH values of root exudates of white lupin plants at 28 DAI. (C,D) Nitrogen (N) and phosphorus (P) concentration in white lupin plants at 28 DAI. (E) Relative quantification of *Bradyrhizobium* in white lupin roots by real-time RT-PCR at 14, 21, and 28 DAI using primers specific for *16S* rRNA gene of *Bradyrhizobium*, using *LaHEL* expression for normalization (E). Letters refer to statistical significance (Holm–Sidak analysis of variance [ANOVA], $n = 3$, p-value <0.05)

characterizing nodules sampled by white lupin plants supplied or not with P, a supervised OPLS-DA analysis was carried out settings two classes (class a: +N+P and −N+P; class b: +N−P and −N−P). For each class, specific variables (macro- and micronutrients) were selected evaluating the S-plots (Figures S5–S7). Class-specific variables were validated by *t*-test analysis. By these analyses, P and Fe

TABLE 1 Element concentrations in white lupin plants (nodules, roots, and shoots; $n = 3$, mean ± SD)

µg g^{-1} DW	B	Mn	Cu	Fe	Zn	Se
Nodule						
+N+P	916.54 ± 741.65	28.20 ± 4.40	31.81 ± 3.02	472.44 ± 65.81	214.25 ± 100.74	5.34 ± 5.67
−N+P	272.77 ± 102.91	19.86 ± 1.15	43.42 ± 4.83	421.12 ± 17.59	268.19 ± 43.49	1.30 ± 0.58
+N−P	323.42 ± 77.18	21.84 ± 6.72	36.36 ± 2.15	652.17 ± 108.33	196.44 ± 27.79	0.22 ± 2.11
−N−P	166.37 ± 37.62	23.91 ± 0.69	65.54 ± 2.05	526.84 ± 57.22	338.07 ± 60.95	nd
Root						
+N+P	834.64 ± 676.55	96.57 ± 15.87	70.98 ± 5.46	1293.22 ± 165.02	227.03 ± 26.76	0.46 ± 4.09
−N+P	1166.89 ± 278.30	98.91 ± 15.13	40.86 ± 8.85	387.73 ± 74.64	366.52 ± 60.57	3.69 ± 3.31
+N−P	718.38 ± 113.13	94.82 ± 16.39	60.48 ± 24.77	662.64 ± 227.29	163.02 ± 123.75	3.47 ± 1.14
−N−P	376.30 ± 99.31	107.52 ± 14.01	50.19 ± 0.08	391.12 ± 44.54	351.37 ± 54.98	1.59 ± 4.37
Shoot						
+N+P	174.00 ± 16.67	799.32 ± 227.14	118.05 ± 95.46	124.17 ± 12.08	82.28 ± 0.42	5.23 ± 1.59
−N+P	133.54 ± 72.67	940.22 ± 96.47	112.07 ± 158.52	167.49 ± 18.89	82.68 ± 40.03	1.93 ± 2.94
+N−P	47.98 ± 23.36	1054.60 ± 60.83	22.86 ± 20.28	177.49 ± 11.37	27.33 ± 22.31	nd
−N−P	nd	1442.68 ± 146.39	17.38 ± 4.25	164.76 ± 11.92	25.16 ± 23.62	1.85 ± 3.92

mg g^{-1} DW	Mg	K	Ca	P	N	C
Nodule						
+N+P	2.12 ± 0.28	69.44 ± 9.08	0.74 ± 0.56	16.35 ± 1.67	/	/
−N+P	2.00 ± 0.06	71.17 ± 2.64	0.45 ± 0.21	17.49 ± 0.42	/	/
+N−P	5.34 ± 1.37	68.01 ± 5.92	0.55 ± 0.25	4.411 ± 0.13	/	/
−N−P	2.07 ± 0.33	63.05 ± 3.49	0.40 ± 0.15	5.96 ± 0.29	/	/
Root						
+N+P	2.23 ± 0.26	44.66 ± 3.21	0.90 ± 0.15	8.94 ± 0.83	33.41 ± 0.69	442.08 ± 2.75
−N+P	1.05 ± 0.05	55.62 ± 7.46	0.34 ± 0.56	14.50 ± 0.63	23.07 ± 1.67	433.60 ± 7.55
+N−P	6.64 ± 1.53	39.22 ± 6.16	0.49 ± 0.10	1.74 ± 0.70	32.71 ± 0.90	440.38 ± 3.16
−N−P	1.25 ± 0.02	48.11 ± 4.36	0.35 ± 0.14	2.06 ± 0.53	26.4 ± 3.21	448.20 ± 4.89
Shoot						
+N+P	3.39 ± 0.47	44.92 ± 4.70	1.94 ± 0.47	6.23 ± 0.66	51.66 ± 1.86	459.42 ± 10.31
−N+P	3.36 ± 0.11	52.32 ± 0.40	1.02 ± 0.19	8.24 ± 0.88	32.25 ± 2.70	442.35 ± 4.85
+N−P	3.41 ± 0.35	55.70 ± 9.26	0.99 ± 0.10	1.45 ± 0.40	47.04 ± 1.18	446.30 ± 0.92
−N−P	3.58 ± 0.18	63.69 ± 5.37	1.23 ± 0.06	1.68 ± 0.15	39.52 ± 4.54	455.82 ± 7.10

Abbreviations: DW, dry weight; nd, not detected.

concentrations were identified as class a- and class b-specific variables, respectively (Table S2).

Root and shoot ionomic datasets were analysed using the same approach applied for the nodule dataset. Regarding root dataset, PCA analysis identified three clusters (Figures 4 and S8–S10). The first principal component splits the samples based on the P supply with the highest separation between roots of plants grown without N or P in nutrient solution (−N+P and +N−P). A three-classes OPLS-DA analysis coupled with *t*-test validation allowed to identify P as the specific variable for plants supplied with P but without N (−N+P; Table S4, Figures S8–S10), while Mg characterized the samples grown with N and without P (+N−P).

PCA analysis carried out for the shoot dataset (Figure 4) evidenced a sample clustering depending on P availability. In shoots, P, Zn and B were identified as variables specific for plants supplied with P (+N+P and −N+P; Table S2, Figures S11–S13). The shoots of plants grown without P were characterized by higher levels of K and Mn (Table S2). The PCA models obtained for nodule, root, and shoot datasets suggest that samples were clustering according to P supply (this trend was particularly evident for nodules and shoots). Under same P nutritional condition (in P sufficiency: +N+P and −N+P conditions; or in P deficiency: +N−P and −N−P conditions), some differences in macro- and micronutrient concentrations were also detectable depending on the N-form available for plants (deriving from the symbiotic N_2-fixation plus or minus the addition of an inorganic N source in nutrient solution; Tables S3 and S4). When P was available, significant variations in Mn and Cu concentrations in nodules were observed depending on N availability in nutrient solution (+N+P nodules showed higher Mn concentration than −N+P, whereas −N+P nodules showed higher

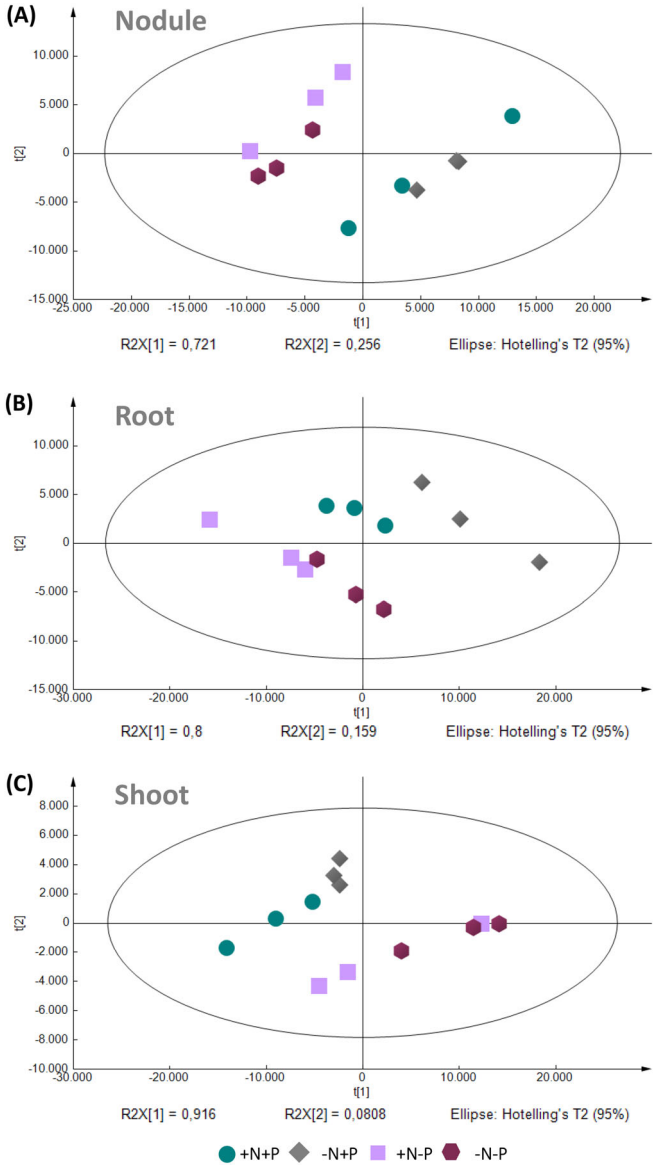

FIGURE 4 Ionomic analyses in white lupin plants at 28 days after inoculation (DAI) under the different nutrient conditions (+N+P, −N+P, +N−P, −N−P). (A) Principal component analysis (PCA) scatterplot representing the 12 samples of nodule (R2: 0.977; Q2: 0.871). (B) PCA scatterplot representing the 12 samples of roots (R2: 0.0097; Q2: 0.773). (C) PCA scatterplot representing the 12 samples of shoots (R2: 0.977; Q2: 0.861). Green circle: +N+P samples; rose box: +N−P; grey diamond: −N+P; purple hexagon: −N−P

Cu concentration than +N+P; Table S3). In roots, the presence of N in nutrient solution (+N+P) increased Fe, N, Mg, and Cu concentrations compared to −N+P plants, while −N+P roots showed an increase of P and Zn (in comparison to +N+P roots). The shoots of plants supplied with N in nutrient solution displayed higher concentration of N and Ca (+N+P in comparison −N+P). On the other hand, N-free nutrient solution induced an increase of P and Fe in this organ (−N+P vs. +N+P). Under P starvation, Mg and B showed higher levels in nodules when N was applied to the nutrient solution (+N−P vs. −N−P); Cu, P, and Zn were higher in nodules of −N−P plants (−N−P vs. +N+P; Table S4). In roots of +N−P plants, higher concentrations of N, Mg, and B were measured compared to −N−P. In shoots, plants grown on N-containing media (+N−P) showed a higher concentration of B and N and a lower concentration of Mn and Ca than −N−P shoots.

3.4 | Gene expression analyses

Real-time RT-PCR analyses allowed us to monitor the gene expression values during the plant growing under different nutritional conditions. Then, 16 genes coding for 4 transporters (DEGRADATION OF UREA, DUR3; PHOSPHATE 1, PHO1; putative citrate transporter, MATE3; putative genistein transporter, MATE2), 9 metabolic enzymes (SUCROSE SYNTHASE 4, SS4; PHOSPHOFRUCTOKINASE 3, PFK; PHOSPHOENOLPYRUVATE CARBOXYLASE, PEPC; MALATE DEHYDROGENASE, MDH; MALATE SYNTHASE, MS; ATP-CITRATE LYASE A-1, CL; Urease, Urease; GLUTAMINE SYNTHETASE 2, GS2; GLUTAMINE-DEPENDENT ASPARAGINE SYNTHASE 1, ASN1) and for 3 enzymes related to root activity (PURPLE ACID PHOSPHATASE 10, PAP10; FERRIC REDUCTION OXIDASE 2, FRO2; H^+-ATPase 2, AHA2), all involved in N, P, and Fe acquisition, were analysed in white lupin roots at 14, 21, and 28 DAI (Figure 5 and Table S5).

At 14 DAI, in roots of plants grown without N in nutrient solution (−N+P), the expression of *LaASN1*, *LaPAP10*, *LaFRO2* was downregulated and that of *LaMATE3* was upregulated, in comparison to +N+P roots. In contrast, P shortage (+N−P) caused only weak transcriptional changes. The absence of both nutrients in the solution upregulated the expression of *LaPAP10* and *LaMATE3*, and downregulated the expression of *LaASN1* and *LaFRO2* (−N−P vs. + N+P).

At 21 DAI, the expression of *LaMS*, *LaPAP10*, and *LaMATE3* was higher in −N−P white lupin than in +N+P and in −N+P plants (with the following gene expression pattern −N−P > −N+P > +N+P). P deficiency (+N−P) induced the expression of *LaMS*, *LaASN1*, *LaPAP10*, *LaFRO2*, and *LaAHA2*, especially the two genes, *LaMS* and *LaPAP10*, were particularly upregulated in roots of +N−P plants than in −N−P ones. The −N−P condition upregulated the expression of *LaPFK* and *LaFRO2* and this modulation was not induced by the other conditions.

At 28 DAI, the expression of some genes known to be involved in N, P, and Fe acquisition (*LaMS*, *LaDUR3*, *LaPAP10*, *LaPHO1*, *LaFRO2*, *LaAHA2* and *LaMATE3*, *LaPEPC*, *LaASN1*, *LaGS2)* was higher in −N−P white lupin than in −N+P and + N+P plants; except for *LaMATE3*, all these genes were upregulated in roots of +N−P plants than in −N−P ones (with the following gene expression pattern +N−P > −N−P > −N+P = +N+P).

3.5 | Fe(III)-chelate reductase activity

The multivariate statistics on the nutritional status of plants showed significant changes for Fe concentration in white lupin organs. Therefore, the capability of the whole root system of white lupin to reduce the

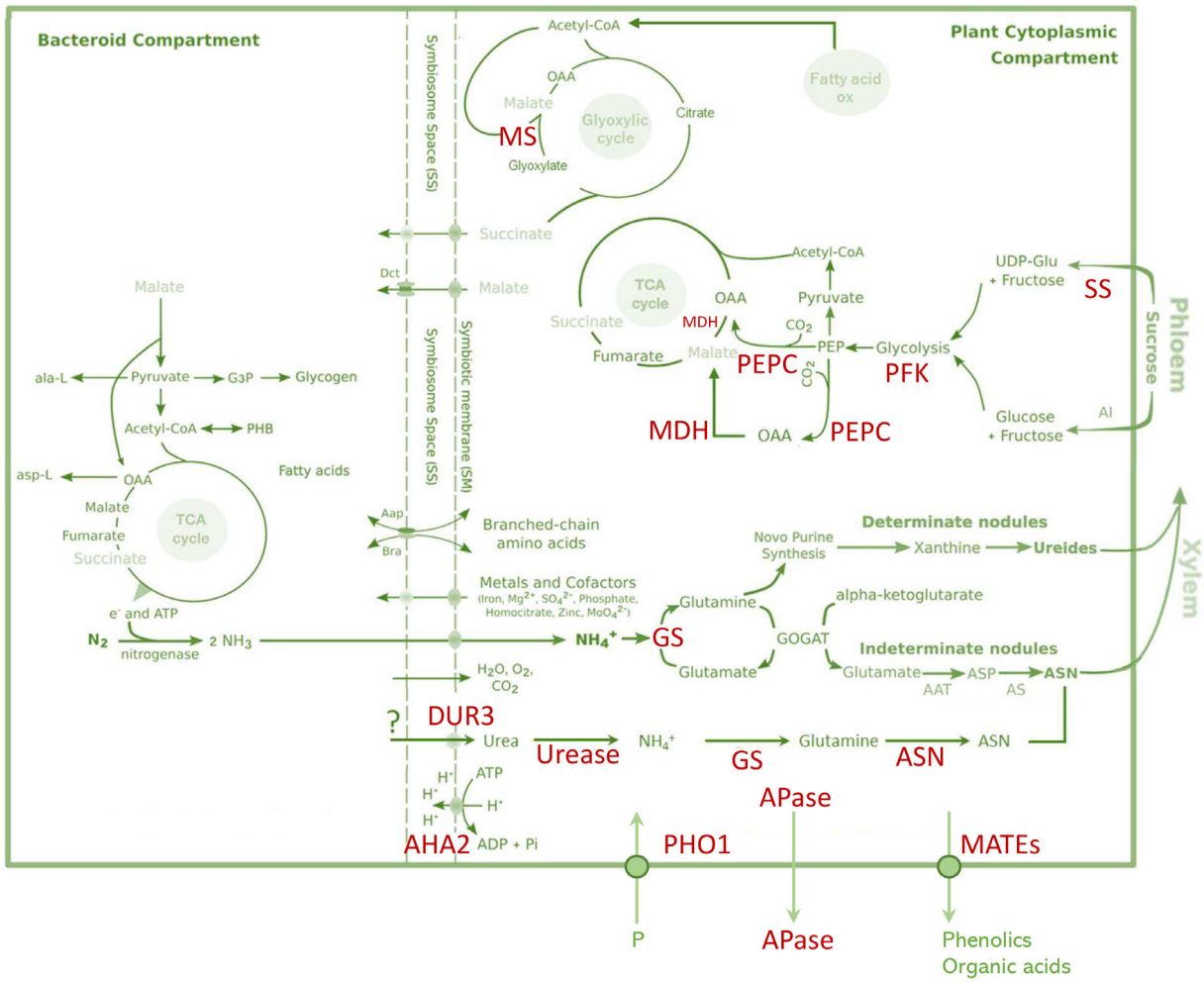

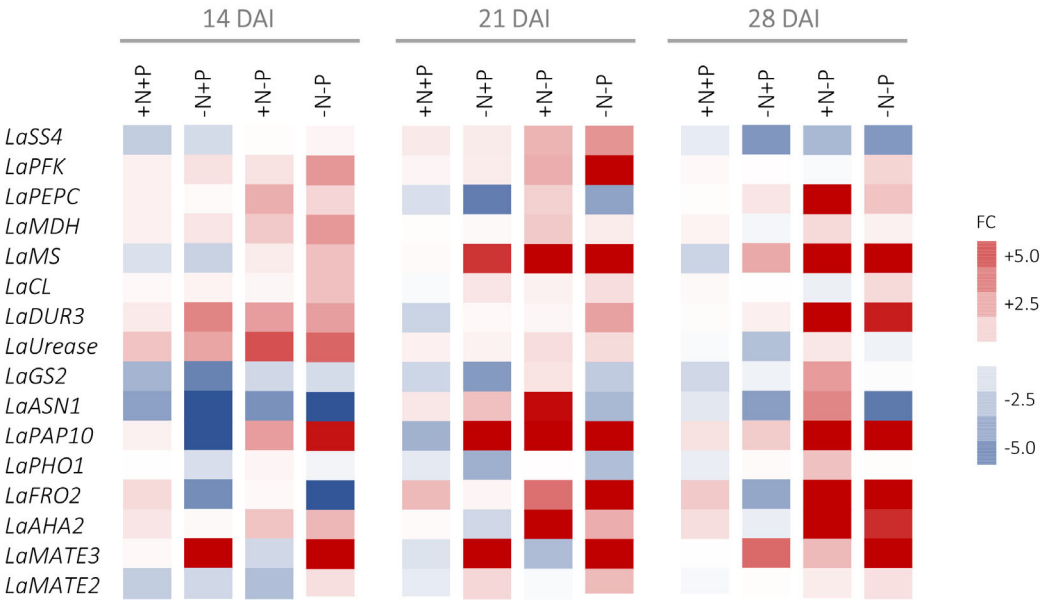

FIGURE 5 (A) Schematic representation of C, N, and P metabolism in nodulated root cell (modified from Liu et al., 2018). (B) Expression of genes involved in N and P acquisition in whole white lupin roots at 14, 21, and 28 days after inoculation (DAI) by real-time RT-PCR. Data indicate the fold change in comparison to one replicate of +N+P roots used as reference (value = 1); red, upregulated genes; blue, downregulated ones. Averages and standard deviations of real-time RT-PCR data are reported in Table S5

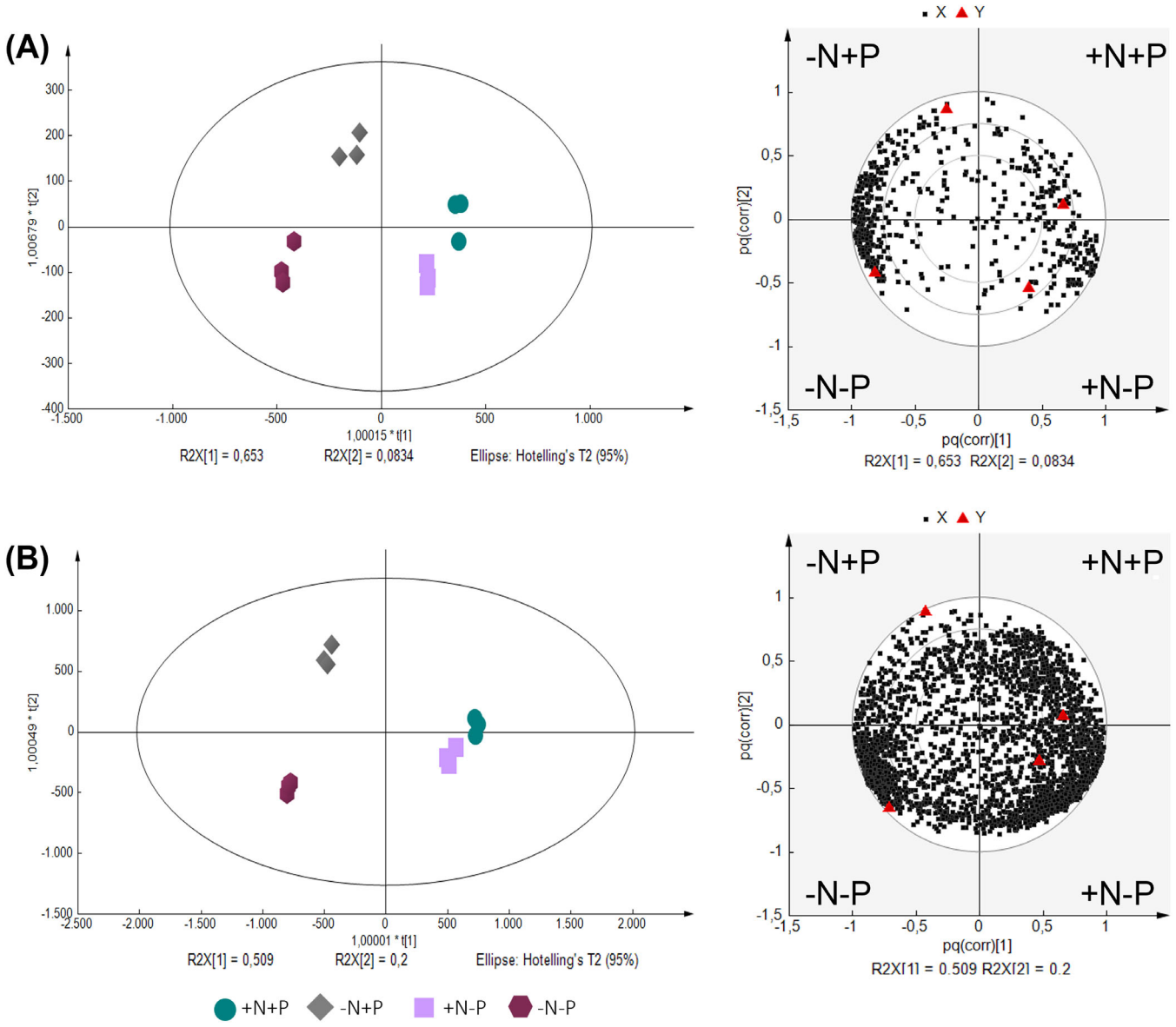

FIGURE 6 Orthogonal partial least square discriminant analysis, score plot (OPLS-DA, on the left) and loading plot (pq(corr)1 vs. pq(corr)2, on the right) from untargeted metabolomic analyses of white lupin root exudates at 28 days after inoculation (DAI). Analyses obtained by negative (A) and positive (B) ionization. In the loading plots, black dots refer to metabolites; red dots refer to four treatments

ferric form to ferrous one was analysed at 28 DAI (Figure S4). The +N−P white lupin roots showed the highest Fe^{III}-chelate reductase activity, while the lowest reduction occurred in −N−P white lupin roots.

3.6 | Untargeted metabolomic analyses of root exudates

The LC–MS analyses provided two data matrices (obtained by positive and negative ionization modes, Table S6) that were explored by OPLS-DA (Figure 6). The samples were clearly clustered according to the nutritional regime (+N+P, −N+P, +N−P, −N−P), with −N+P much different from the other three groups, and the two groups +N+P and +N−P close to each other but still distinguishable. The loading plot showed that the group −N+P was mainly negatively characterized by lower metabolite level, while −N−P from one side and + N+P/+N−P from the other side were positively characterized by the higher level of many metabolites. Thus, the availability of N in the nutrient solution was the strongest factor affecting the exudate metabolome composition. In house and public database comparison of metabolite masses allowed to find the elemental composition of 58 *m/z* features in the negative ionization and 69 *m/z* features in positive ionization dataset, based on accurate mass and isotope similarity. Unfortunately, the precise identification of these metabolites through the fragmentation patterns and comparison with authentic standards, when available, gave few positive results. Despite the elemental composition precisely corresponding to known and common flavonoids

TABLE 2 Untargeted metabolomic analyses of root exudates of lupin plants at 28 DAI under different nutritional treatments. The putatively identified metabolites belonged to three groups of compounds: (1) nucleosides monophosphates and their precursors; (2) saponins; (3) flavonoids. Colour scale refers to the relative level of each metabolite within a row (red colour, high level; white colour, low level). The metabolite levels are expressed in arbitrary units and represent the average ± standard deviation of the peak areas extrapolated from three biological replicates. Statistically significant differences among the conditions were indicated by a different letter (Holm–Sidak ANOVA, $n = 3$, p-value <0.05)

Group	ID	Elemental composition	Putative identification accepted	Average ± standard deviation				Significance			
				+N+P	−N+P	+N−P	−N−P	+N+P	−N+P	+N−P	−N−P
Group 1	1706	$C_{10}H_{13}N_5O_4$	Adenosine	407.94 ± 106.24	986.87 ± 572.82	518.15 ± 141.22	436.21 ± 104.69	a	a	a	a
	1594	$C_9H_{12}N_2O_6$	Uridine (sodium adduct)	0.00 ± 0.00	36.04 ± 17.37	0.59 ± 1.03	94.88 ± 9.72	c	b	cd	a
	1711	$C_5H_5N_5O$	Guanine	16.28 ± 1.77	104.57 ± 39.80	23.74 ± 4.82	48.85 ± 19.76	b	a	b	ab
	1647	$C_{10}H_{14}N_5O_7P$	AMP	134.91 ± 24.43	380.16 ± 52.03	95.63 ± 12.87	341.58 ± 118.68	b	a	b	a
	1704	$C_{10}H_{14}N_5O_7P$	AMP	31.80 ± 11.10	476.61 ± 352.45	1.25 ± 1.25	279.35 ± 63.54	a	a	a	a
	1670	$C_{10}H_{14}N_5O_8P$	GMP	27.16 ± 6.66	255.34 ± 171.84	20.41 ± 5.67	574.82 ± 253.66	b	ab	b	a
	1710	$C_{10}H_{14}N_5O_8P$	GMP	5.41 ± 6.42	184.05 ± 134.67	0.00 ± 0.00	150.33 ± 35.60	a	a	a	a
	170	$C_9H_{13}N_2O_9P$	UMP	0.30 ± 0.53	560.74 ± 220.97	0.00 ± 0.00	739.57 ± 383.83	b	ac	bc	a
	198	$C_9H_{13}N_2O_9P$	UMP	16.19 ± 11.16	257.62 ± 145.78	1.54 ± 1.31	264.26 ± 39.86	b	a	b	a
Group 2	2745	$C_{48}H_{78}O_{18}$	Soyasaponin I (soyasapogenol E + glucuronic acid–galactose–rhamnose)	5390.97 ± 2354.84	19116.50 ± 6517.37	12316.66 ± 10400.72	24923.25 ± 7230.31	a	a	a	a
	2611	$C_{54}H_{88}O_{23}$	Soyasaponin I glucoside (sodium adduct)	2996.23 ± 129.21	8792.56 ± 3552.82	7627.45 ± 1952.72	13339.08 ± 1654.65	b	ab	b	a
	2574	$C_{54}H_{88}O_{23}$	Soyasaponin I glucoside (sodium adduct)	27.72 ± 4.66	89.11 ± 30.72	73.09 ± 22.71	142.72 ± 22.52	c	ab	bc	a
	2593	$C_{36}H_{56}O_9$	Soyasapogenol E glucuronide	632.86 ± 511.23	3813.67 ± 903.49	1928.29 ± 1417.43	7647.11 ± 1220.11	c	b	bc	a
	2856	$C_{36}H_{56}O_9$	Soyasapogenol E glucuronide	559.36 ± 402.78	1223.94 ± 223.76	2293.46 ± 1504.53	2035.93 ± 383.25	a	a	a	a
	482	$C_{54}H_{86}O_{23}$	Soyasapogenol E + glucose–glucose–rhamnose–glucuronic acid	5023.91 ± 1082.12	64108.41 ± 21899.04	26286.14 ± 7418.69	118220.64 ± 15461.44	c	b	c	a
Group 3	452	$C_{16}H_{12}O_7$	Isorhamnetin (tetrahydroxy methoxyflavone) or structural isomer	2.21 ± 2.09	498.56 ± 16.16	2.64 ± 1.26	573.95 ± 198.25	b	a	b	a
	431	$C_{16}H_{12}O_7$	Tetrahydroxy methoxyflavone	9.13 ± 9.73	3219.17 ± 365.43	8.17 ± 6.46	2755.40 ± 967.24	b	a	b	a
	428	$C_{15}H_{10}O_6$	Hydroxygenistein	10.57 ± 3.87	1890.25 ± 312.70	8.93 ± 1.89	3552.11 ± 1468.57	c	ab	bc	a
	2381	$C_{24}H_{22}O_{13}$	Genistein-O-glucoside malonylated	576.83 ± 239.08	234.66 ± 104.10	1269.88 ± 576.32	327.89 ± 128.25	ab	b	a	b
	2349	$C_{24}H_{22}O_{13}$	Genistein-O-glucoside malonylated	21.49 ± 7.16	140.83 ± 76.54	103.58 ± 40.66	296.87 ± 202.90	a	a	a	a
	2264	$C_{34}H_{36}O_{22}$	Chrysoeriol-O-diglucoside-dimalonylated	2.11 ± 1.97	78.11 ± 31.03	4.59 ± 6.72	316.30 ± 6.63	c	b	c	a
	2148	$C_{33}H_{34}O_{21}$	Genistein-O-diglucoside dimalonylated	1.10 ± 1.90	189.19 ± 96.74	29.96 ± 28.29	491.08 ± 99.85	c	b	c	a
	2338	$C_{33}H_{34}O_{21}$	Genistein-O-diglucoside dimalonylated	1.50 ± 2.61	57.02 ± 9.18	51.88 ± 46.54	204.32 ± 9.18	b	b	b	a

Abbreviations: ANOVA, analysis of variance, DAI, days after inoculation.

(as flavones, flavanones, and isoflavones), the fragmentation spectrum and/or the retention time did not. We cannot exclude that the detected metabolites are structural isomers of known metabolites, for which the authentic standards and thus the fragmentation patterns are not available.

The putatively identified metabolites belonged to three groups of compounds: (1) nucleosides monophosphates and their precursors; (2) saponins; (3) flavonoids (Table 2).

Group 1 included guanine, uridine, adenosine, and two structural isomers of GMP, UMP, and AMP (maybe corresponding to the nucleoside-5′-monophosphate and nucleoside-3′-monophosphate). An overall increase of these metabolites characterized the exudates collected from plants grown in the absence of N in the nutrient solution (−N+P and −N−P) compared to those grown in the presence of N (+N+P and +N−P; Table 2).

Group 2 included soyasapogenol B conjugated with the *O*-glycan glucuronic acid-galactose-rhamnose (soyasaponin I), two isomers of the same molecule with a further hexose sugar, soyasapogenol E conjugated with *O*-hexose-hexose-desoxyhexose-glucuronic acid, two isomers of soyasapogenol E conjugated with glucuronic acid. A gradual increase of saponin levels was observed from +N+P samples to +N−P, followed by −N+P and with the highest level in −N−P samples (Table 2). They were identified based on accurate mass and on fragmentation: soyasapogenol B derivative contained the fragment 459.3838 corresponding to aglycone, and the fragments 441.373, 423.362, and 405.352 corresponding to sequential dehydration of aglycone, as described by Tsuno et al. (2018), while symmetrically, soyasapogenol E-based soyasaponins contained the fragments 457.3681, 439.357, 421.347, and 403.336. Moreover, the fragmentation patterns of the metabolites putatively annotated as soyasaponin I and soyasaponin I hexoside (which is soyasapogenol B derivative) showed exactly the fragmentation pattern already reported for this saponin (Taylor et al., 2009).

Group 3 included various isoflavones (hydroxygenistein, genistein-*O*-glucoside, and di-glucoside malonylated and di-malonylated), the flavonol isorhamnetin and one isorhamnetin structural isomer (tehrahydroxy methoxyflavone) and the flavone chrysoeriol diglucoside dimalonylated. All these metabolites, except the two genistein-*O*-glucoside malonylated, were more abundant in the exudates of the -N samples (isorhamnetin and its structural isomer, hydroxygenistein) or in the exudates of −N−P samples (genistein and chrysoeriol *O*-diglucoside dimalonylated). The two genistein-*O*-glucoside malonylated apparently showed a different behaviour, but the very high standard deviation prevented having a clear picture of these two metabolites (Table 2).

Though the analytical method was not specific for polar metabolites, such as sugars and organic acids, we were still able to observe the signals of citrate and isocitrate in the root exudates of −N−P samples. For each metabolite, the relative level is expressed in arbitrary unit and was calculated based on the peak area in the ion chromatogram: 3290.50 ± 816.71 relative level of citric acid (formula $C_6H_8O_7$, *m/z* detected: 191.0185); 25.05 ± 17.05 relative level of isocitric acid (formula $C_6H_8O_7$, *m/z* detected: 191.0192).

4 | DISCUSSION

In the present work, the physiological and molecular responses of white lupin plants were analysed during symbiosis with *Bradyrhizobium* sp. (*Lupinus*). At the end of the growing period (28 DAI), typical symptoms of N- and P-limiting conditions were visible on −N+P and +N−P plants, respectively. Morphological and morphometric adaptations (e.g. the formation of nodules and cluster roots, acidification/alkalinization of the root external media) of white lupin plants agree with previous results (Müller et al., 2015; Schulze et al., 2006). As white lupin is a model plant for tolerance to low-P stress and usually establish symbiotic interaction with N_2-fixing bacteria, no changes of plant DWs were observed among conditions (as observed comparing P-deficient and P-sufficient non-nodulating white lupin plants published in Zanin et al., 2019). The simultaneous absence of N and P from the nutrient solution (−N−P) induced plants symptoms characterized by intermediate values of SPAD index, shoot N concentration and nodule P concentration between −N+P and +N−P (Figures 1 and 3). In addition, −N−P plants had the tendency to form high number of nodules, to increase the dry matter of nodules and to promote the growth of *Bradyrhizobium* compared to the other conditions (Figure S2). These data suggest that −N−P condition can stimulate the activity of N_2-fixation needed to sustain plant growth (Schulze et al., 2006).

4.1 | Acidification of the root external solution and primary metabolism

The −N−P condition induced the strongest acidification of the root external solution, which might be related to an unbalanced cations acquisition rather than anions when nitrate is absent from the nutrient solution (Hinsinger et al., 2003; Tang & Rengel, 2002). Moreover, the assimilation of ammonium (produced by nodule and assimilated in roots) and the release of root exudates might contribute to the acidification of the root external solution (Feng et al., 2020). This evidence suggests that in −N−P roots, a peculiar response in terms of plant nutrient composition and metabolomic pattern of the root exudome might occur.

Macro- and micronutrient concentrations of inoculated white lupin plants were mainly affected by P rather than N availability in nutrient solution (Figure 4, Table S2). These results agree with previous evidence (Sas et al., 2002) showing that shoot levels of K and Mn under P deficiency were enhanced. The release of H^+ and organic acids by P-deficient cluster roots promotes the Mn mobilization in the rhizosphere and stimulates the Mn and K uptake in plants (Briskin & Gawienowski, 1996; Hawkesford et al., 2012; Pang et al., 2018). At the molecular level, the acidification processes of the rhizosphere are mainly linked to the internal pH-stat mechanism mainly operated by the activity of two enzymes (PEPC and MDH). In agreement with Schulze et al. (2006), our data indicates that at the end of the growing period (28 DAI), the P deficiency induced the gene expression of *LaPEPC*, contributing to the acidification around mature cluster roots (for cluster stages, see Massonneau et al., 2001). Maybe even more relevant, these two enzymes are involved in the synthesis of organic acids, which are needed to meet the demand of C by rhizobial bacteroids and

are highly released under P-deficiency (Britto & Kronzucker, 2005). In fact, one-third of the exuded carbon in P-deficient white lupin roots derived from PEPC activity (Johnson, Allan, et al., 1996; Johnson, Vance, & Allan, 1996). Under −N−P, the gene expression of *LaPEPC* and *LaMDH* were not induced in white lupin roots, but the gene coding for the upstream glycolytic enzyme PFK was highly induced (at 21 DAI) and these data are in agreement with the key role of PPi-PFK activity as metabolic bypass when P is limiting (Plaxton & Tran, 2011). Moreover, according to the intense release of citrate and isocitrate by −N−P roots (see Section 3), −N−P white lupin roots induced the expression of a putative transporter mediating the root release of citrate *LaMATE3* (Gottardi, 2012).

4.2 | The activation of the PSR

Coherently with PSR, the expression of genes involved in the synthesis of malate and APs (*LaMS* and *LaPAP10*) were induced by P starvation (in +N−P and −N−P roots) and they were also upregulated when N was missing from the nutrient solution (−N+P). This evidence suggests that −N−P nodulating white lupin plants share mechanisms between PSR and N-metabolism to meet the P demand and therefore guarantee the proceeding of N_2-fixation processes. The release of phenolic compounds is functional to maximize nutrient bioavailability in the rhizosphere. The exudation of flavonoids and isoflavonoids is essential for the establishment of symbiosis between rhizobia and legume plants (Biala-Leonhard et al., 2021; Liu & Murray, 2016; Subramanian et al., 2006) and are active in the modulation of soil microorganism activities (Cesco et al., 2010; Tomasi et al., 2008). The gene expression analysis of a putative genistein efflux transporter (*LaMATE2*; Biala-Leonhard et al., 2021) agrees with the high release of genistein derivatives in −N−P plants, suggesting that plants were active to promote the establishment of symbiosis with rhizobium under this condition. Therefore, depending on nutrient availability, the transcriptional pattern of *LaMATEs* (*LaMATE2* and *LaMATE3*) might be crucial to determine the quality and quantity of the root exudome to promote plant–soil–microbe interactions.

4.3 | N acquisition pathway: the effect of P deficiency on the expression of urea transporter

In the last years, the occurrence of a regulatory network that integrates the nitrate and P starvation signals has been identified (Medici et al., 2015), and this signalling network orchestrates the spatial arrangement of root architecture depending on N and P availability (Shahzad & Amtmann, 2017). As hypothesized by Krouk and Kiba (2020), the upregulation of some genes coding for N-transport and N-assimilatory enzymes under P deficiency (+N−P and −N−P: upregulation of urea transporter, *LaDUR3*; +N−P: upregulation of ammonium assimilation, *LaGS2* and *LaASN1*; Figure 5) suggests the occurrence of this regulatory network. To the best of our knowledge, no previous evidence related urea acquisition to P availability. Under P starvation, the acquisition of urea as N source might allow better control of internal cellular pH than the N-inorganic sources. The acquisition of organic-low MW N-molecules by cluster roots was previously described in white lupin (Hawkins et al., 2005). Another hypothesis may consider the involvement of *LaDUR3* on N-remobilization processes occurring in cluster roots, especially in the senescent stages. This response may provide new insights into the physiological role of this transporter and might give the reason for the higher N allocation in shoots of −N−P plants in comparison to −N+P.

4.4 | Plant Fe and Cu nutritional status

In nodulating plants, the Fe nutritional status is a crucial factor for some metabolic processes, including N_2-fixation and nitrate reduction processes (Brear et al., 2013; Nikolic et al., 2007; Slatni et al., 2009). The highest value of Fe concentration in +N+P roots and the low expression of *LaAHA2* and *LaFRO2* genes agree with an adequate Fe nutritional level in +N+P plants that did not need the activation of Fe starvation response. Vice versa, the poor availability of Fe or P reciprocally activates molecular systems for their acquisition, proofing the occurrence of an interplay between these two nutrients (Valentinuzzi et al., 2019; Venuti et al., 2019; Zanin et al., 2017). The strategies operated by plants to cope with Fe starvation share some mechanisms with those operated under P starvation. Our results show that under P deficiency (+N−P and −N−P plants), the upregulation of the genes *LaAHA2* and *LaFRO2*, known to be involved in iron acquisition, takes place. This response was confirmed by an increase of FRO activity in +N−P roots (Figure S4). Among the other factors, P solubility in the soil is greatly dependent on Fe. Therefore, the activation of FRO by P shortage can represent a valid strategy operated by plants to prevent Fe co-precipitation with P ensuring at the same time the acquisition of the metal by roots. Indeed, the Fe concentration in +N−P white lupin roots was higher than in no-nitrate-treated ones. It is interesting to note that in −N−P, the upregulation of *LaFRO2* was not followed by an increase of enzymatic activity (Figures 5 and S4). Although a post-transcriptional regulation of this latter enzyme is not excluded (Connolly et al., 2002), we suppose that under −N−P condition the reduction of ferric to ferrous form can be mainly sustained by phenolic compounds (having reducing capacity). In fact, through reduction and complexation, these compounds promote the solubility of nutrients, such as Fe and P from sparingly soluble forms. These molecules (along with nucleosides monophosphates and soyasaponins) were highly abundant in the −N−P root exudome, in agreement with the high abundance of *LaMATE2* expression (Table 2).

The activity of *Bradyrhizobium* sp. (*Lupinus*) in nodules seems to be related to the nutritional levels of copper (Cu, Seliga, 1999; Sánchez-Pardo et al., 2012). The Cu metallochaperones are involved in the assembly of cytochrome C oxidase, an enzyme playing a role in N_2-fixation in soybean nodules (Arunothayanan et al., 2010; Serventi et al., 2012). Moreover, in nodules, N_2-fixation is linked to melanin, which synthesis involves a Cu-containing enzyme (polyphenol oxidase; Seliga, 1993; Cubo et al., 1988). Our results indicate that under no-nitrate treatment (N derived only by N_2-fixation processes), the Cu concentration in nodules increased independently to the P availability.

4.5 | Nucleosides monophosphates in the root exudates

Nucleosides monophosphates (including their precursors) mainly characterized the white lupin-roots exudome when N was missing from nutrient solution and were also highly released under −N−P condition. Some works provided evidence that the nucleotide and nucleoside metabolism is activated in nodules (Delmotte et al., 2010; Vauclare et al., 2013) where purines and pyrimidines were accumulated (Barsch et al., 2006; Lardi et al., 2016). These compounds can be released by roots (Dakora & Phillips, 2002), but their physiological role has not yet been elucidated. Due to high N and P content, it is plausible that these molecules can represent a nutrient source at the rhizosphere, useful to sustain the growth and development of microorganisms (Dakora & Phillips, 2002). Based on our data, we can suppose that these exudates can promote a synergistic action between plants and rhizospheric microbes, promoting the growth of bacteria and fungi communities that carry out a beneficial role to improve nutrient availability for plants.

4.6 | Soyasaponins in the root exudates

Untargeted analyses also identified various soyasaponins derived from soyasapogenol B and soyasapogenol E, decorated with oligosaccharide moieties. Soyasaponins are widespread within legume species, including white lupin, as reported by Singh et al. (2017). Many roles have been attributed to soyasaponins, including allelopathic properties and roles in plant defence against fungi, bacteria, insects, and other plant predators (Mugford & Osbourn, 2013). In *Medicago*, the overexpression of a gene encoding for a key enzyme of triterpene saponin biosynthesis from *Aster sedifolius* (*AsOXA1*, β-amyrin synthase) caused an increase of soyasaponins and root nodules (Confalonieri et al., 2009), suggesting a positive role of soyasapogenol derivatives on nodulation. Soyasaponins have been recently found in some legume species, including soybean, *Medicago sativa*, *Lotus japonicus*, *Pisum sativum*, also in the root exudates (Tsuno et al., 2018). However, to the best of our knowledge, this is the first report of soyasaponins in the root exudates of white lupin. In soybean, the amount of soyasaponins in root exudates changed with the age of the plants (Tsuno et al., 2018). Moreover, one of the soyasaponin was shown to diffuse over longer distances in the rhizosphere than daidzein and to affect the bacterial communities by increasing the populations of potential plant growth-promoting rhizobacteria (Fujimatsu et al., 2020). Here, we showed that the secretion of soyasaponins in white lupin was strongly related to nutritional stress since they increased both under −N+P and +N−P conditions compared to +N+P plants. There was even an additive effect when both N and P were absent in nutrient solution (−N−P plants). Under our experimental conditions, where plants were inoculated with a specific bacteria strain, −N−P plants showed the highest *Bradyrhizobium* number (Figure 3). Thus, it could be speculated that depending on nutritional status, plants can stimulate a molecular cross talk between roots and bacteria mediated by soyasaponin,

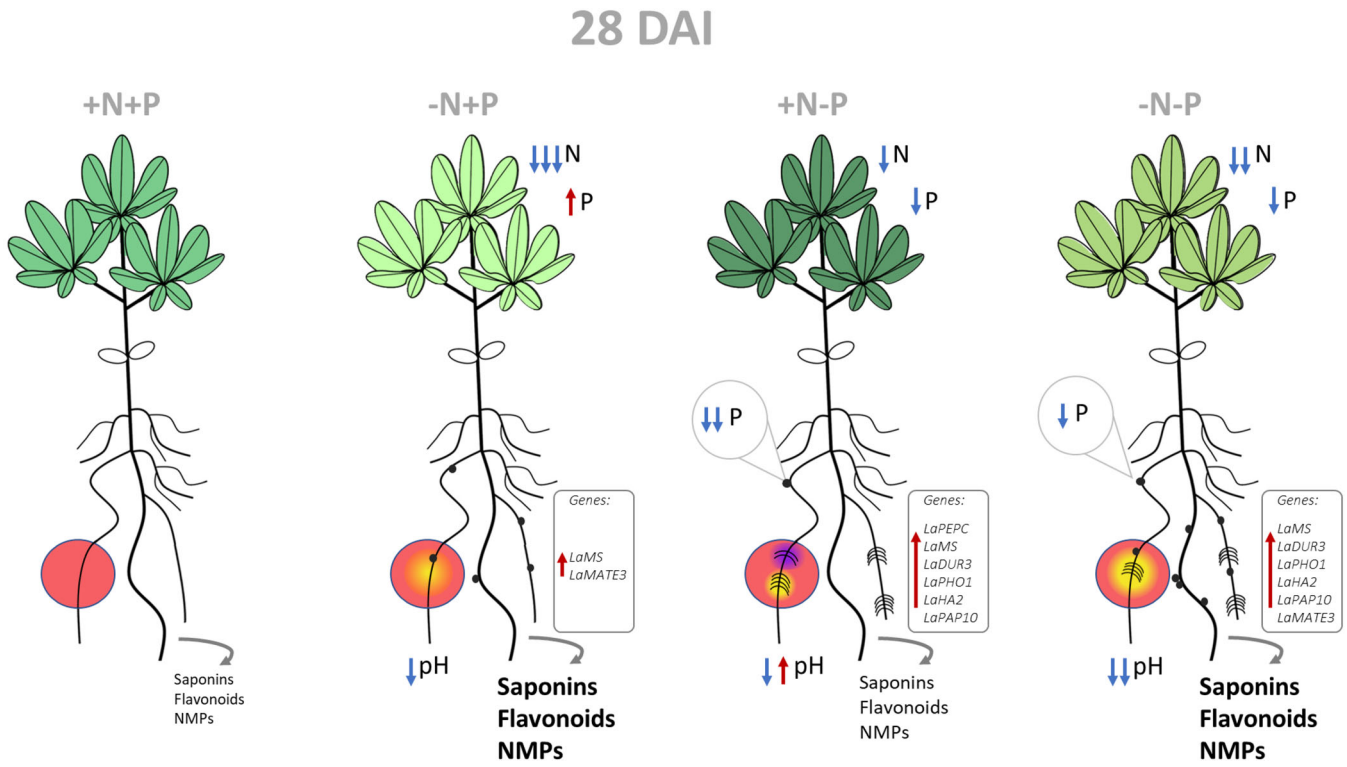

FIGURE 7 Schematic representation of changes occurring at white lupin root system (lupin plant was drawn by Müller et al., 2015)

which could be beneficial for the bacterial communities helping plants to improve growth and mineral balance under such conditions.

5 | CONCLUSIONS

This study shows that, in white lupin, the simultaneous starvation of N and P in nutrient solution induced the activation of specific responses characterized by an intense reprogramming of metabolic processes in nodulating roots. The ionomic and transcriptional changes suggest the occurrence of a synergistic action between N and P nutritional pathways that interplayed to counteract the nutritional shortage of the external solution. It cannot be excluded that translocation and allocation processes might have a crucial role in coping with −N−P condition, promptly redistributing nutrients in the whole plant and therefore guaranteeing a maximum efficiency of the metabolic machinery. Besides, the untargeted analyses of root exudome highlighted the relevance of such known and unknown compounds to cope with nutritional disorders (e.g. flavonoids, nucleosides, and saponins; Figure 7).

ACKNOWLEDGEMENT

The *Bradyrhizobium* sp. (*Lupinus*) strain was a kind gift of Dr José J. Pueyo (Centro de Ciencias Medioambientales, CSIC, Madrid, Spain). Open Access Funding provided by Universita degli Studi di Udine within the CRUI-CARE Agreement. [Correction added on 17 May 2022: CRUI-CARE funding statement has been added.]

CONFLICT OF INTEREST

The authors declare no conflict of interest.

AUTHOR CONTRIBUTIONS

Sara Buoso and Anita Zamboni: Performed the experiments, analysed and interpreted the results and wrote the manuscript. Alessandro Franco: Performed ionomic experiments and revised the manuscript. Mauro Commisso and Flavia Guzzo: Performed metabolomic experiments, interpreted the results and revised the manuscript. Zeno Varanini and Roberto Pinton: Interpreted the results and revised the manuscript. Nicola Tomasi: Analysed and interpreted the results and revised the manuscript. Laura Zanin: Conceived and supervised the experiments, performed the experiments, analysed and interpreted the results and wrote the manuscript. All authors read and approved the final manuscript.

DATA AVAILABILITY STATEMENT

The data that support the findings of this study are available in the supplementary material of this article.

ORCID

Laura Zanin https://orcid.org/0000-0002-3840-9843

REFERENCES

Al-Niemi, T.S., Kahn, M.L. & McDermott, T.R. (1997) P metabolism in the bean-Rhizobium tropici symbiosis. *Plant Physiology*, 113, 1233–1242.

Al-Niemi, T.S., Kahn, M.L. & McDermott, T.R. (1998) Phosphorus uptake by bean nodules. *Plant and Soil*, 198, 71–78.

Arunothayanan, H., Nomura, M., Hamaguchi, R., Itakura, M., Minamisawa, K. & Tajima, S. (2010) Copper metallochaperones are required for the assembly of bacteroid cytochrome c oxidase which is functioning for nitrogen fixation in soybean nodules. *Plant and Cell Physiology*, 51, 1242–1246.

Barsch, A., Tellstrom, V., Patschkowski, T., Kuster, H. & Niehaus, K. (2006) Metabolite profiles of nodulated alfalfa plants indicate that distinct stages of nodule organogenesis are accompanied by global physiological adaptations. *Molecular Plant-Microbe Interactions*, 19, 998–1013.

Biala-Leonhard, W., Zanin, L., Gottardi, S., de Brito Francisco, R., Venuti, S., Valentinuzzi, F. et al. (2021) Identification of an isoflavonoid transporter required for the nodule establishment of the Rhizobium-Fabaceae symbiotic interaction. *Frontiers in Plant Science*, 12, 758213. https://doi.org/10.3389/fpls.2021.758213

Brear, E.M., Day, D.A. & Smith, P.M. (2013) Iron: an essential micronutrient for the legume-rhizobium symbiosis. *Frontiers in Plant Science*, 4, 359.

Briskin, D.P. & Gawienowski, M.C. (1996) Role of the plasma membrane H+-ATPase in K+ transport. *Plant Physiology*, 111(4), 1199–1207.

Britto, D.T. & Kronzucker, H.J. (2005) Nitrogen acquisition, PEP carboxylase, and cellular pH homeostasis: new views on old paradigms. *Plant, Cell & Environment*, 28, 1396–1409.

Buoso, S., Tomasi, N., Said-Pullicino, D., Arkoun, M., Yvin, J.C., Pinton, R. et al. (2021) Characterization of physiological and molecular responses of *Zea mays* seedlings to different urea-ammonium ratios. *Plant Physiology and Biochemistry*, 162, 613–623.

Cesco, S., Neumann, G., Tomasi, N., Pinton, R. & Weisskopf, L. (2010) Release of plant-borne flavonoids into the rhizosphere and their role in plant nutrition. *Plant and Soil*, 329, 1–25.

Chu, Q., Sha, Z., Maruyama, H., Yang, L., Pan, G., Xue, L. et al. (2019) Metabolic reprogramming in nodules, roots, and leaves of symbiotic soybean in response to iron deficiency. *Plant, Cell & Environment*, 42, 3027–3043.

Commisso, M., Negri, S., Bianconi, M., Gambini, S., Avesani, S., Ceoldo, S. et al. (2019) Untargeted and targeted metabolomics and tryptophan decarboxylase in vivo characterization provide novel insight on the development of kiwifruits (*Actinidia deliciosa*). *International Journal of Molecular Sciences*, 20, 897.

Confalonieri, M., Cammareri, M., Biazzi, E., Pecchia, P., Salema Fevereiro, M.P., Balestrazzi, A. et al. (2009) Enhanced triterpene saponin biosynthesis and root nodulation in transgenic barrel medic (*Medicago truncatula* Gaertn.) expressing a novel β-amyrin synthase (*AsOXA1*) gene. *Plant Biotechnology Journal*, 7, 172–182.

Connolly, E.L., Fett, J.P. & Guerinot, M.L. (2002) Expression of the IRT1 metal transporter is controlled by metals at the levels of transcript and protein accumulation. *Plant Cell*, 14, 1347–1357.

Cubo, M.T., Buendia-Claveria, A.M., Beringer, J.E. & Ruiz-Sainz, J.E. (1988) Melanin production by Rhizobium strains. *Applied and Environmental Microbiology*, 54, 1812–1817.

Dakora, F.D. & Phillips, D.A. (2002) Root exudates as mediators of mineral acquisition in low-nutrient environments. *Plant and Soil*, 245, 35–47.

Delmotte, N., Ahrens, C.H., Knief, C., Qeli, E., Koch, M., Fischer, H.M. et al. (2010) An integrated proteomics and transcriptomics reference data set provides new insights into the *Bradyrhizobium japonicum* bacteroid metabolism in soybean root nodules. *Proteomics*, 10, 1391–1400.

Dinkelaker, B., Römheld, V. & Marschner, H. (1989) Citric acid excretion and precipitation of calcium citrate in the rizosphere of white lupin (*Lupinus albus* L.). *Plant, Cell & Environment*, 12, 285–292.

Feng, H., Fan, X., Miller, A.J. & Xu, G. (2020) Plant nitrogen uptake and assimilation: regulation of cellular pH homeostasis. *Journal of Experimental Botany*, 71, 4380–4392.

Fujimatsu, T., Endo, K., Yazaki, K. & Sugiyama, A. (2020) Secretion dynamics of soyasaponins in soybean roots and effects to modify the bacterial composition. *Plant Direct*, 4, e00259.

Gardner, W.K., Barber, D.A. & Parbery, D.G. (1983) The acquisition of phosphorus by *Lupinus albus* L. III. The probable mechanism by which phosphorus movement in the soil/root interface is enhanced. *Plant and Soil*, 70, 391–402.

Gardner, W.K., Parbery, D.G. & Barber, D.A. (1982) The acquisition of phosphorus by *Lupinus albus* L. I. Some characteristics of the soil/root interface. *Plant and Soil*, 67, 19–32.

González-Sama, A., Lucas, M.M., De Felipe, M.R. & Pueyo, J.J. (2004) An unusual infection mechanism and nodule morphogenesis in white lupin (*Lupinus albus*). *New Phytologist*, 163, 371–380.

Gottardi, S. (2012) *Studio fisiologico e molecolare dei meccanismi di rilascio di essudati radicali e dell'assorbimento di Fe e P*. PhD thesis, Udine University. Available from https://air.uniud.it/retrieve/handle/11390/1132541/250240/10990_79_TesiStefanoGottardi.pdf [Accessed March 2012].

Hawkesford, M., Horst, W., Kichey, T., Lambers, H., Schjoerring, J., Skrumsager Møller, I. et al. (2012) Chapter 6—functions of macronutrients. In: Marschner, P. (Ed.) *Marschner's mineral nutrition of higher plants*, 3rd edition. Amsterdam, The Netherlands: Academic Press, pp. 135–189.

Hawkins, H.J., Wolf, G. & Stock, W.D. (2005) Cluster roots of *Leucadendron laureolum* (Proteaceae) and *Lupinus albus* (Fabaceae) take up glycine intact: an adaptive strategy to low mineral nitrogen in soils? *Annals of Botany*, 96, 1275–1282.

Hinsinger, P., Plassard, C., Tang, C. & Jaillard, B. (2003) Origins of root-mediated pH changes in the rhizosphere and their responses to environmental constraints: a review. *Plant and Soil*, 248, 43–59.

Høgh-Jensen, H., Schjoerring, J.K. & Soussana, J.-F. (2002) The influence of phosphorus deficiency on growth and nitrogen fixation of white clover plants. *Annals of Botany*, 90, 745–753.

Johnson, J.F., Allan, D.L., Vance, C.P. & Weiblen, G. (1996) Root carbon dioxide fixation by phosphorus-deficient *Lupinus albus*. Contribution to organic acid exudation by proteoid roots. *Plant Physiology*, 112, 19–30.

Johnson, J.F., Vance, C.P. & Allan, D.L. (1996) Phosphorus deficiency in *Lupinus albus*. Altered lateral root development and enhanced expression of phosphoenolpyruvate carboxylase. *Plant Physiology*, 112, 31-41. Lupin (*Lupinus albus* L.) grown under phosphorus-deficient conditions? *Plant and Cell Physiology*, 46, 892–901.

Johnston, A.E., Poulton, P.R., Fixen, P.E. & Curtin, D. (2014) Phosphorus: its efficient use in agriculture. *Advances in Agronomy*, 123, 177–228.

Jordan, D.C. (1984) Bradyrhizobium. In: *Bergey's manual of systematic bacteriology*. Baltimore, MD: Williams &Wilkins, pp. 242–244.

Koressaar, T. & Remm, M. (2007) Enhancements and modifications of primer design program Primer3. *Bioinformatics*, 23, 1289–1291.

Krouk, G. & Kiba, T. (2020) Nitrogen and phosphorus interactions in plants: from agronomic to physiological and molecular insights. *Current Opinion in Plant Biology*, 57, 104–109.

Lardi, M., Murset, V., Fischer, H.M., Mesa, S., Ahrens, C.H., Zamboni, N. et al. (2016) Metabolomic profiling of *Bradyrhizobium diazoefficiens*-induced root nodules reveals both host plant-specific and developmental signatures. *International Journal of Molecular Sciences*, 17, 815.

Le Roux, M.R., Khan, S. & Valentine, A.J. (2008) Organic acid accumulation may inhibit N_2 fixation in phosphorus-stressed lupin nodules. *New Phytologist*, 177, 956–964.

Le Roux, M.R., Ward, C.L., Botha, F.C. & Valentine, A.J. (2006) Routes of pyruvate synthesis in phosphorus-deficient lupin roots and nodules. *New Phytologist*, 169, 399–408.

Liu, A., Contador, C.A., Fan, K. & Lam, H. (2018) Interaction and regulation of carbon, nitrogen, and phosphorus metabolisms in root nodules of legumes. *Frontiers in Plant Science*, 9, 1860.

Liu, C.W. & Murray, J.D. (2016) The role of flavonoids in nodulation host-range specificity: an update. *Plants (Basel, Switzerland)*, 5, 33.

Liu, J., Uhde-Stone, C., Li, A., Vance, C. & Allan, D. (2001) A phosphate transporter with enhanced expression in proteoid roots of white lupin (*Lupinus albus* L.). *Plant and Soil*, 237, 257–266.

Livak, K.J. & Schmittgen, T.D. (2001) Analysis of relative gene expression data using real time quantitative PCR and the $2^{-\Delta\Delta Ct}$ method. *Methods*, 25, 402–408.

Massonneau, A., Langlade, N., Leon, S., Smutny, J., Vogt, E., Neumann, G. et al. (2001) Metabolic changes associated with cluster root development in white lupin (*Lupinus albus* L.): relationship between organic acid excretion, sucrose metabolism and energy status. *Planta*, 213, 534–542.

Medici, A., Marshall-Colon, A., Ronzier, E., Szponarski, W., Wang, R., Gojon, A. et al. (2015) AtNIGT1/HRS1 integrates nitrate and phosphate signals at the Arabidopsis root tip. *Nature Communications*, 6, 1–11.

Mugford, S.T. & Osbourn, A. (2013) Saponin synthesis and function. In: Bach, T.J. & Rohmer, M. (Eds.) *Isoprenoid synthesis in plants and microorganisms*. New York, NY: Springer, pp. 405–424.

Müller, J., Gödde, V., Niehaus, K. & Zörb, C. (2015) Metabolic adaptations of white lupin roots and shoots under phosphorus deficiency. *Frontiers in Plant Science*, 6, 1014.

Neumann, G., Massonneau, A., Martinoia, E. & Römheld, V. (1999) Physiological adaptations to phosphorus deficiency during proteoid root development in white lupin. *Planta*, 208, 373–382.

Nikolic, M., Cesco, S., Römheld, V., Varanini, Z. & Pinton, R. (2007) Short-term interactions between nitrate and iron nutrition in cucumber. *Functional Plant Biology*, 34, 402–408.

Pang, J., Ruchi, B., Zhao, H., Bansal, R., Bohuon, E., Lambers, H. et al. (2018) The carboxylate-releasing phosphorus-mobilising strategy could be proxied by foliar manganese concentration in a large set of chickpea germplasm under low phosphorus supply. *New Phytologist*, 219, 518–529.

Plaxton, W.C. & Tran, H.T. (2011) Metabolic adaptations of phosphate-starved plants. *Plant Physiology*, 156, 1006–1015.

Pueyo, J.J., Quiñones, M.A., Coba De La Peña, T., Fedorova, E.E. & Lucas, M.M. (2021) Nitrogen and phosphorus interplay in lupin root nodules and cluster roots. *Frontiers in Plant Science*, 12, 184.

Qin, L., Wang, M., Chen, L., Liang, X., Wu, Z., Lin, Z. et al. (2015) Soybean Fe–S cluster biosynthesis regulated by external iron or phosphate fluctuation. *Plant Cell Reports*, 34, 411–424.

Ritz, C. & Spiess, A.N. (2008) qpcR: an R package for sigmoidal model selection in quantitative real-time polymerase chain reaction analysis. *Bioinformatics*, 24, 1549–1551.

Sadowsky, M.J., Tully, R.E., Cregan, P.B. & Keyser, H.H. (1987) Genetic diversity in *Bradyrhizobium japonicum* serogroup 123 and its relation to genotype-specific nodulation of soybean. *Applied and Environmental Microbiology*, 53, 2624–2630.

Sánchez-Pardo, B., Fernández-Pascual, M. & Zornoza, P. (2012) Copper microlocalisation, ultrastructural alterations and antioxidant responses in the nodules of white lupin and soybean plants grown under conditions of copper excess. *Environmental and Experimental Botany*, 84, 52–60.

Sas, L., Rengel, Z. & Tang, C. (2002) The effect of nitrogen nutrition on cluster root formation and proton extrusion by *Lupinus albus*. *Annals of Botany*, 89, 435–442.

Schulze, J., Temple, G., Temple, S.J., Beschow, H. & Vance, C.P. (2006) Nitrogen fixation by white lupin under phosphorus deficiency. *Annals of Botany*, 98, 731–740.

Seliga, H. (1993) The role of copper in nitrogen fixation in *Lupinus luteus* L. *Plant and Soil*, 155, 349–352.

Seliga, H. (1999) Antioxidative activity of copper in root nodules of yellow lupin plants. *Acta Physiologiae Plantarum*, 21, 427–431.

Serventi, F., Youard, Z.A., Murset, V., Huwiler, S., Bühler, D., Richter, M. et al. (2012) Copper starvation-inducible protein for cytochrome oxidase biogenesis in *Bradyrhizobium japonicum*. *The Journal of Biological Chemistry*, 287, 38812–38823.

Shahzad, Z. & Amtmann, A. (2017) Food for thought: how nutrients regulate root system architecture. *Current Opinion in Plant Biology*, 39, 80–87.

Shane, M.W. & Lambers, H. (2005) Cluster roots: a curiosity in context. *Plant and Soil*, 274, 101–125.

Singh, B., Singh, J.P., Singh, N. & Kaur, A. (2017) Saponins in pulses and their health promoting activities: a review. *Food Chemistry*, 233, 540–549.

Slatni, T., Krouma, A., Gouia, H. & Abdelly, C. (2009) Importance of ferric chelate reductase activity and acidification capacity in root nodules of N_2-fixing common bean (*Phaseolus vulgaris* L.) subjected to iron deficiency. *Symbiosis*, 47, 35–42.

Subramanian, S., Stacey, G. & Yu, O. (2006) Endogenous isoflavones are essential for the establishment of symbiosis between soybean and *Bradyrhizobium japonicum*. *The Plant Journal*, 48, 261–273.

Syers, J.K., Johnston, A.E. & Curtin, D. (2008) *Efficiency of soil and fertilizer phosphorus use: reconciling changing concepts of soil phosphorus behaviour with agronomic information*. Rome: Food and Agriculture Organization of the United Nations.

Tang, C., Hinsinger, P., Drevon, J.J. & Jaillard, B. (2001) Phosphorus deficiency impairs early nodule functioning and enhances proton release in roots of *Medicago truncatula* L. *Annals of Botany*, 88, 131–138.

Tang, C. & Rengel, Z. (2002) Role of plant cation/anion uptake ratio in soil acidification. In: Rengel, Z. (Ed.) *Handbook of soil acidity*. New York: Marcel Dekker.

Taylor, C.M., Jost, R., Erskine, W. & Nelson, M.N. (2016) Identifying stable reference genes for qRT-PCR normalisation in gene expression studies of narrow-leafed lupin (*Lupinus angustifolius* L.). *PLoS One*, 11, e0148300.

Taylor, W.G., Sutherland, D.H. & Richards, K.W. (2009) Soyasaponins and related glycosides of *Desmodium canadense* and *Desmodium illinoense*. *The Open Natural Products Journal*, 2, 59–67.

Thuynsma, R., Valentine, A. & Kleinert, A. (2014) Phosphorus deficiency affects the allocation of below-ground resources to combined cluster roots and nodules in *Lupinus albus*. *Journal of Plant Physiology*, 171, 285–291.

Tomasi, N., Weisskopf, L., Renella, G., Landi, G., Pinton, R., Varanini, Z. et al. (2008) Flavonoids of white lupin roots participate in phosphorus mobilization from soil. *Soil Biology and Biochemistry*, 40, 1971–1974.

Tsuno, Y., Fujimatsu, T., Endo, K., Sugiyama, A. & Yazaki, K. (2018) Soyasaponins: a new class of root exudates in soybean (*Glycine max*). *Plant Cell Physiology*, 59, 366–375.

Untergrasser, A., Cutcutache, I., Koressaar, T., Ye, J., Faircloth, B.C., Remm, M. et al. (2012) Primer3-new capabilities and interfaces. *Nucleic Acids Research*, 40, e115.

Valentinuzzi, F., Venuti, S., Pii, Y., Marroni, F., Cesco, S., Hartmann, F. et al. (2019) Common and specific responses to iron and phosphorus deficiencies in roots of apple tree (*Malus× domestica*). *Plant Molecular Biology*, 101, 129–148.

Vance, C.P., Uhde-Stone, C. & Allan, D.L. (2003) Phosphorus acquisition and use: critical adaptations by plants for securing a non-renewable resource. *New Phytologist*, 157, 423–447.

Vauclare, P., Bligny, R., Gout, E. & Widmer, F. (2013) An overview of the metabolic differences between *Bradyrhizobium japonicum* 110 bacteria and differentiated bacteroids from soybean (*Glycine max*) root nodules: an in vitro 13C- and 31P-nuclear magnetic resonance spectroscopy study. *FEMS Microbiology Letters*, 343, 49–56.

Venuti, S., Zanin, L., Marroni, F., Franco, A., Morgante, M., Pinton, R. et al. (2019) Physiological and transcriptomic data highlight common features between iron and phosphorus acquisition mechanisms in white lupin roots. *Plant Science*, 285, 110–121.

Wang, X., Ding, W. & Lambers, H. (2019) Nodulation promotes cluster-root formation in *Lupinus albus* under low phosphorus conditions. *Plant and Soil*, 439, 233–242.

Weisskopf, L., Tomasi, N., Santelia, D., Martinoia, E., Langlade, N.B., Tabacchi, R. et al. (2006) Isoflavonoid exudation from white lupin roots is influenced by phosphate supply, root type and cluster-root stage. *New Phytologist*, 171, 657–668.

Zamboni, A., Zanin, L., Tomasi, N., Pezzotti, M., Pinton, R., Varanini, Z. et al. (2012) Genome-wide microarray analysis of tomato roots showed defined responses to iron deficiency. *BMC Genomics*, 13, 1–14.

Zanin, L., Tomasi, N., Zamboni, A., Sega, D., Varanini, Z. & Pinton, R. (2018) Water-extractable humic substances speed up transcriptional response of maize roots to nitrate. *Environmental and Experimental Botany*, 147, 167–178.

Zanin, L., Tomasi, N., Zamboni, A., Varanini, Z. & Pinton, R. (2015) The urease inhibitor NBPT negatively affects DUR3-mediated uptake and assimilation of urea in maize roots. *Frontiers in Plant Science*, 6, 1007.

Zanin, L., Venuti, S., Marroni, F., Franco, A., Morgante, M., Pinton, R. et al. (2019) Physiological and RNA sequencing data of white lupin plants grown under Fe and P deficiency. *Data in Brief*, 28(25), 104069.

Zanin, L., Venuti, S., Zamboni, A., Varanini, Z., Tomasi, N. & Pinton, R. (2017) Transcriptional and physiological analyses of Fe deficiency response in maize reveal the presence of strategy I components and Fe/P interactions. *BMC Genomics*, 18, 1–15.

SUPPORTING INFORMATION

Additional supporting information may be found in the online version of the article at the publisher's website.

How to cite this article: Buoso, S., Zamboni, A., Franco, A., Commisso, M., Guzzo, F., Varanini, Z. et al. (2022) Nodulating white lupins take advantage of the reciprocal interplay between N and P nutritional responses. *Physiologia Plantarum*, 174(1), e13607. Available from: https://doi.org/10.1111/ppl.13607